

Deposition of small Cu, Ag and Au particles on reduced SiO₂

R.M. Ferullo^{*}, G.R. Garda, P.G. Belelli, M.M. Branda, N.J. Castellani^{*}

Grupo de Materiales y Sistemas Catalíticos, Departamento de Física, Universidad Nacional del Sur, Avenida Alem 1253, 8000 Bahía Blanca, Buenos Aires, Argentina

Received 6 October 2005; accepted 6 March 2006

Available online 23 May 2006

Abstract

In this work, the adsorption of M_n (M: Cu, Ag, Au; n = 1–3) particles on the ≡Si–O· defect of a SiO₂ surface is studied in the framework of density functional theory. A charge transfer from the metal particle to the support is observed following the sequence: Cu ≈ Ag > Au. This is in agreement with the greater ionization potential of the latter metal. The M₁–M_{n–1}OSi≡ and M_n–OSi≡ interactions of nucleation and adhesion processes, respectively, were analyzed from an energetic point of view. The strongest interaction is obtained always between two open-shell systems. When the comparison is performed among the metals, the bond strength of the M–M interaction follows the order: Cu ≈ Au > Ag. The deep position of Ag d-levels in the energy scale could explain the relatively weak Ag–Ag interaction. If the M–oxide interaction is considered, this order in the bond strength was observed: Cu > Ag > Au. The strong adhesion for Cu could be ascribed to the greater charge transfer to the support and to a strong Cu(d)–O(p) interaction. On the other hand, for Au the charge transfer to the support is relatively small, while for Ag the Ag(d)–O(p) interaction is relatively weak due to the more localized Ag(d) band.

© 2006 Elsevier B.V. All rights reserved.

Keywords: Cu/SiO₂; Ag/SiO₂; Au/SiO₂; Metal small particles; Metal–support interaction; Density functional theory

1. Introduction

The study of the metal/oxide interface represents a field of wide interest in different industrial areas such as catalysis, gas sensors, electrochemistry and microelectronics. In particular, in heterogeneous catalysis the oxide acts as a support where the metal particles grow. The reactivity of the metal aggregates strongly depends on the cluster size, which in turn depends on the nature of point or extended defects where the particle anchors. Thus, the role of the support material is more important than initially thought.

Cu, Ag and Au-based catalysts have been studied for a wide variety of reactions. For instance, supported Cu catalysts are used for methanol synthesis, oxidation of hydrocarbons and hydrogenation reactions [1–4]. The activity of catalysts based on Ag has been examined for the catalytic reduction of NO_x [5,6]. Dispersed ultrafine Au particles on oxides exhibit an extraordinarily high activity for low-temperature catalytic combustion, partial oxidation of hydrocarbons and

hydrogenation of unsaturated hydrocarbons [7]. On the other hand, Cu, Ag and Au were used as promoters on the activity and selectivity of Pt and Pd-based catalysts [8,9].

Quantum-chemical studies of the deposition of small metal particles on oxide surfaces are important to get an accurate description of the initial stages of interface formation. For instance, Lopez et al. analyzed the Cu deposition on silica using the DFT formalism [10,11]. They found that the regular sites of the silica surface are unreactive toward metal particles. In contrast, defect sites like the nonbridging oxygen, ≡Si–O·, and the Si dangling bond, ≡Si· (the ≡ symbol indicates the three Si–O bonds), are very reactive and they are probably centers where the nucleation takes place [12,13]. These centers were detected on the surface of dehydroxylated or mechanically activated silica [14]. In a previous work, it was shown that ≡Si–O· sites react more strongly with Cu atoms than the terminal ≡Si· defects [15]. Concerning the chemical reactivity of these Cu particles, it was observed that the support may strongly alter the bonding between the metal and adsorbates such as NCO, H₂ and CO [15–18].

Recently, the deposition of Cu, Ag and Au atoms on different oxides was studied from a theoretical point of view using both cluster and periodic slabs models. For Cu and Ag adsorption on rutile TiO₂(110) surface, Giordano et al. have observed an electron charge transfer from the metal atom to the surface, yielding the formation of Cu⁺ and Ag⁺ ions and a

^{*} Corresponding authors. Tel.: +54 291 4595141; fax: +54 291 4595142.

E-mail addresses: caferull@criba.edu.ar (R.M. Ferullo), castella@criba.edu.ar (N.J. Castellani).

consequent strong interaction with the bridging oxygens [19]. In the case of Au atoms, the interaction with the surface is weaker in concordance with a less important charge transfer. Here, the bonding was better described as covalent polar. The adsorption energies follow the order $\text{Cu} > \text{Ag} > \text{Au}$. On the other side, on $\alpha\text{-Al}_2\text{O}_3(0001)$ surface the metal atoms also interact preferentially on oxygen sites, following the order $\text{Cu} > \text{Au} > \text{Ag}$ [20]. The metal–oxide interaction was interpreted in terms of two main factors: the charge transfer to the support and the metal polarization. While for Cu and Ag the largest contribution to the interaction energy arises from the charge transfer to the surface, for Au the bonding is dominated by polarization of the metal.

In this work, a comparative theoretical analysis of the Cu_n , Ag_n and Au_n ($n=1-3$) particles deposition on reduced SiO_2 is performed in the framework of density functional theory (DFT). In our model, only the $\equiv\text{Si}-\text{O}\cdot$ defect site was considered as a possible center where the metal particle grows. The goal is to attain a qualitative description of both the metal–metal and metal–oxide interactions.

2. Computational details

Calculations were carried out in a system consisting of a metal particle, M_n (with $\text{M}=\text{Cu}$, Ag , Au and $n=1-3$), adsorbed on the $\equiv\text{Si}-\text{O}\cdot$ surface defect of silica represented by a cluster model approach. In the past, it was established that the bond formed between Cu and defect sites of the silica surface is very local and even small clusters describe properly the nature of this chemical interaction [11].

Density Functional Theory (DFT) quantum-mechanical calculations were carried out using the gradient corrected Becke's three parameters hybrid exchange functional in combination with the correlation functional of Lee, Yang and Parr (B3LYP) [21]. This method has been widely used to study adsorption processes yielding reliable results both on oxides and metal clusters. The 6-31G(d) basis set was applied on all the atoms belonging to the central tetrahedron, and the 6-31G basis set on those of the peripheral tetrahedrons. For Cu, Ag and Au the LANL2DZ basis set was used.

The SiO_2 surfaces were represented using $\text{Si}_4\text{O}_4(\text{OH})_9$ clusters. The terminal oxygen atoms were saturated with hydrogen atoms. We started with the ideal β -cristobalite structure as initial geometry. The position of surface oxygen defect and the orientation of the peripheral tetrahedrons were fully relaxed (see Fig. 1). For the M_n/SiO_2 systems the metal aggregates were also fully optimized. Geometry optimizations have been performed by means of analytical gradients with no symmetry constraints.

In order to analyze the direct interaction between the metal particles and the surface oxygen defect, the adhesion energy was calculated. Furthermore, the strength of the metal–metal bonding was investigated by means of the nucleation energy. These energies are defined as follows: $E_{\text{adh}} = [E(\text{M}_n/\text{SiO}_2) - E(\text{M}_n) - E(\text{SiO}_2)]$, with $n=1, 2$ or 3 , and $E_{\text{nuc}} = [E(\text{M}_n/\text{SiO}_2) - E(\text{M}_1) - E(\text{M}_{n-1}/\text{SiO}_2)]$, with $n=2$ or 3 , and where $\text{M}=\text{Cu}$, Ag or Au . The adhesion energies for supported

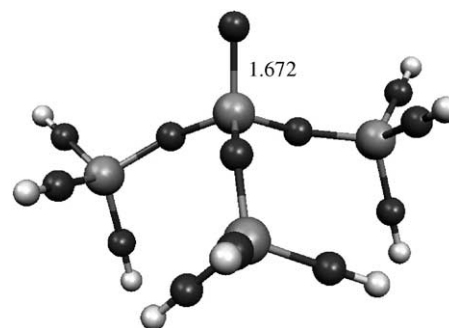


Fig. 1. Optimized geometry of the $\equiv\text{Si}-\text{O}\cdot$ surface defect of silica (distance in Å).

M_3 were calculated considering the isolated M_3 molecule at its triangular structure. Our calculations indicate that the quasi-linear and the triangular structures are very close in energy for the three metals (they differ at most by 0.15 eV).

The interaction energies were corrected by the basis set superposition error (BSSE) using the counter-poise correction [22]. The atomic charges were computed according to the NBO (Natural Bond Orbital) population analysis which is based on quantum perturbation theory [23]. The spin density (SD) is expressed in terms of the Mülliken population analysis [24]. This quantity has demonstrated its usefulness for the characterization of the bond at the interface of similar systems [19]. The calculations have been performed using the Gaussian 03 program package [25].

3. Results and discussion

3.1. Optimized structures and charge transfer

In Fig. 2, the optimized geometries of individual metal atoms interacting with the oxide surface are pictured. The metal atoms adsorb on the $\equiv\text{Si}-\text{O}\cdot$ site forming a $\text{Si}-\text{O}-\text{M}$ angle of nearly 115° . In all the cases, an electron charge transfer from the metal to the support occurs (see Table 1). The values are of 0.7e for Cu and Ag, and of 0.5e for Au in agreement with its poor capability to be oxidized. The charge taken by the support resides mainly on the O of the $\equiv\text{Si}-\text{O}$ group, changing from $-0.6e$ in the defective bare surface to about $-1.2e$ (for Cu and Ag) and $-1.0e$ (for Au) when the metal atoms interact with it.

The optimized geometries of the deposited dimers are represented in Fig. 3. For Cu, an electrostatic interaction takes place between the terminal atom (Cu_B in Fig. 3) and a regular bridging O atom [10,15]. The interaction of Ag_2 with the support produces a different structure with both atoms directly linked with the surface O atom. In contrast, the Au dimer is the only case for which the interaction with the surface is accomplished by means of one metal atom. Similar results were recently found by Antonietti et al. for the adsorption of Au_2 on $\alpha\text{-SiO}_2$ cluster models [26]. The amount of charge transferred to the support is similar to that obtained for the monomer (Table 2). However, the atomic charge distribution is

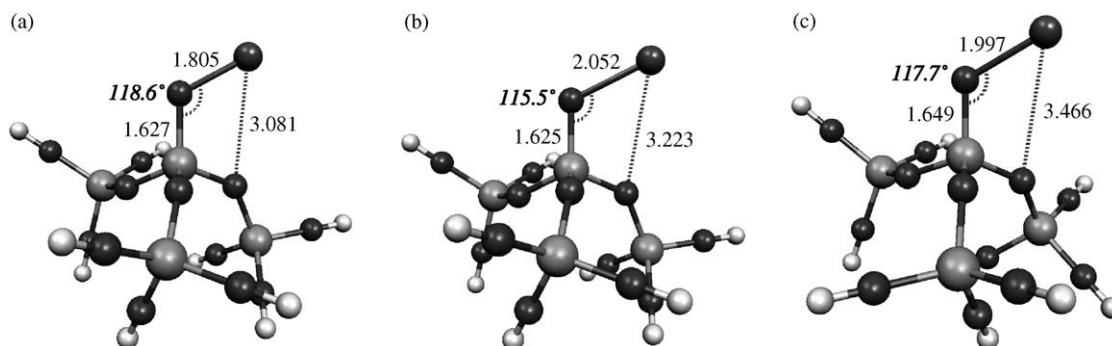


Fig. 2. Structural models of Cu, Ag and Au monomers on the $\equiv\text{Si-O}\cdot$ adsorption site (distances in Å). (a) Cu/SiO₂; (b) Ag/SiO₂; (c) Au/SiO₂.

different for the three cases. For Cu, the atom directly linked to the support has a higher positive charge than the terminal one. In spite of that, the terminal atom (Cu_B) has enough positive charge to establish the above-mentioned electrostatic interaction with a regular O atom of the support. In case of Ag₂, the atomic net charges are similar for both silver atoms owing to its symmetric structure. For Au₂, while the positive charge of the atom directly attached to the support is as high as that obtained for Cu₂, the terminal one is hardly negatively charged.

To study the deposited M₃ particles, the optimization was started positioning the third atom over the optimal dimer structure. This possibility was the only explored, not excluding the existence of other minima on the potential energy surface. The resulting geometries are depicted in Fig. 4. In all the cases quasi-equilateral triangles are formed, which are bonded to the surface similarly than the corresponding dimers. In particular, for the Cu trimer the electrostatic bonding between one Cu atom and a regular O is also present. Interestingly, this bonding is absent when the geometrical structure of SiO₂ is settled to that of the ideal β -cristobalite [17]. The charge transfer from M₃ to the oxide shows similar trends than that of M₂ (Table 3). Although the trimer orientation for Cu and Ag are different, the charge distribution is similar for both metals.

As a measure of the ability of M_n particles to release electronic charge to the silica surface, the vertical ionization potentials (IP) for the isolated metal particles were evaluated and summarized in Table 4. Looking at the corresponding IP values, we observe that the charge transfer to the oxide follows the order Cu \approx Ag > Au, which is in line with the higher IP for the latter metal. Moreover, for the sake of comparison, the experimental values have also been reported in the same table [27–29]. It is noteworthy the very good agreement between both series of data.

Table 1
Adsorption properties of Cu, Ag and Au monomers on the $\equiv\text{Si-O}\cdot$ surface defect

	M ₁ /SiO ₂		
	Cu	Ag	Au
E_{adh} (eV)	−2.92	−2.13	−1.90
$Q(\text{M})$ (a.u.)	0.71	0.70	0.49
$Q(\text{O}_{\text{supp}})$ (a.u.)	−1.22	−1.20	−1.05

3.2. Study of the metal–metal interaction: nucleation energies

The metal–metal interaction was analyzed by means of the nucleation energy concept defined above, i.e. the energy associated with the dimer formation when an isolated metal atom interacts with a preadsorbed atom, and with the trimer formation when an isolated metal atom interacts with a preadsorbed M₂ particle. The values are listed in Tables 2 and 3 and shown as a diagram in Fig. 5. Such a study is relevant to understand the initial stages of a metal particle formation.

Looking at Fig. 5, we observe that the interaction of two open-shell systems is a more favorable situation than the interaction of one open-shell system with a closed-shell one. The former case corresponds to M₃–O–Si \equiv and to free M₂. Here, a direct coupling with two unpaired electrons is produced (M₁· + ·M₂–O–Si \equiv and M₁· + ·M₁, respectively). Conversely, the latter case corresponds to M₂–O–Si \equiv and to free M₃. A closed-shell system has to ‘open’ its configuration in order to form a bond [10]. This seems to be the phenomenon which rules the interaction of fragments if the comparison is based on the type of interacting system, independently of the metal component.

Thus, the noticeable differences between the E_{nucl} values for particles at gas phase and for supported ones in the case of M₁–M₁ and M₂–M₁ interactions are mainly due to the fact that the support ‘changes’ the electronic structure of one of the interacting fragments, from a closed-shell at gas phase to an open-shell when the cluster is supported, or vice versa.

Recently, Wang et al. have studied the electronic structures of isolated Cu₂, Ag₂ and Au₂ using the DFT theory [30]. For Cu₂ and Au₂, they found that the energy gaps between d- and s-molecular orbitals are close and small, which accounts for their similar spectroscopic properties. Conversely, for Ag₂ a small contribution of d electrons to the frontier molecular orbitals was observed owing to the large separation between s- and d-type molecular orbitals. Our results for these molecules follow the same trend (see Fig. 6). In particular, the calculated dissociation energy values follow the order Cu \approx Au > Ag (in magnitude), in line with the experimental results [27] (Table 2). This behaviour could be ascribed to the relatively stronger interaction between d orbitals of Cu and Au, and a relatively weaker interaction between the more localized d orbitals of Ag.

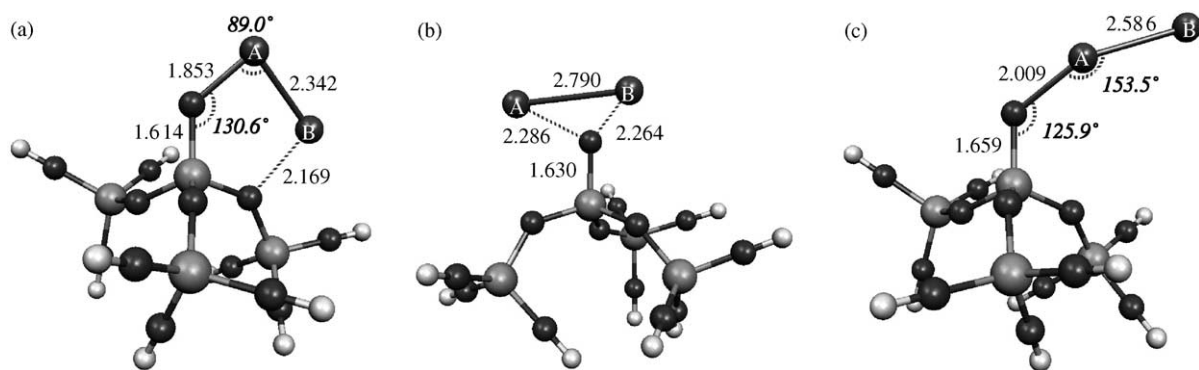


Fig. 3. Structural models of Cu, Ag and Au dimers on the $\equiv\text{Si-O}\cdot$ adsorption site (distances in Å). (a) Cu_2/SiO_2 ; (b) Ag_2/SiO_2 ; (c) Au_2/SiO_2 .

Table 2
Adsorption properties of Cu, Ag and Au dimers on the $\equiv\text{Si-O}\cdot$ surface defect

	M_2/SiO_2		
	Cu	Ag	Au
E_{nucl} (eV)	-0.99 (-1.81) ^a	-0.85 (-1.49) ^a	-1.08 (-1.80) ^a
E_{adh} (eV)	-2.17	-1.54	-1.20
$Q(\text{M}_A)$ (a.u.)	0.46	0.39	0.45
$Q(\text{M}_B)$ (a.u.)	0.25	0.35	-0.07
$Q(\text{M}_2)$ (a.u.)	0.71	0.74	0.38
$Q(\text{O}_{\text{supp}})$ (a.u.)	-1.25	-1.25	-0.98
SD ^b on M_A	0.41	0.41	0.24
SD on M_B	0.43	0.43	0.34
SD on O_{supp}	0.14	0.14	0.40

^a In parentheses, the E_{nucl} of free metal dimers: $E_{\text{nucl}} = [E(\text{M}_2) - 2E(\text{M}_1)]$.

^b SD stands for spin density.

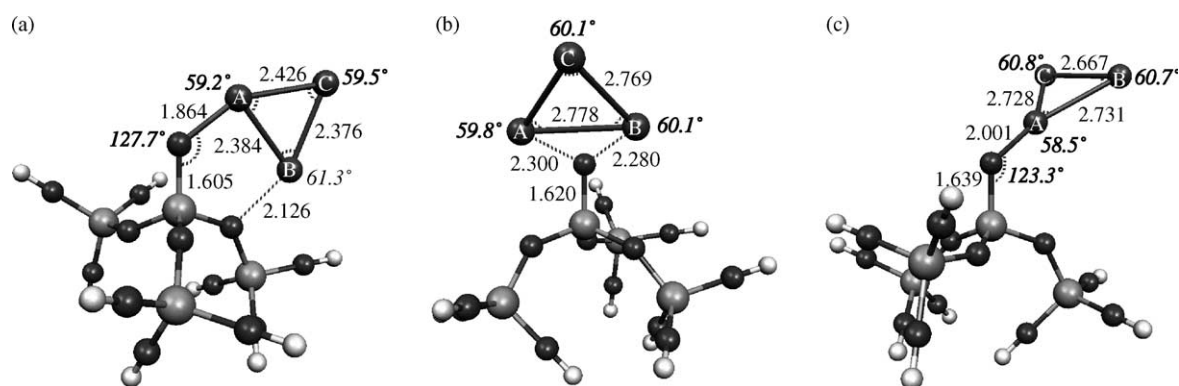


Fig. 4. Structural models of Cu, Ag and Au trimers on the $\equiv\text{Si-O}\cdot$ adsorption site (distances in Å). (a) Cu_3/SiO_2 ; (b) Ag_3/SiO_2 ; (c) Au_3/SiO_2 .

Table 3
Adsorption properties of Cu, Ag and Au trimers on the $\equiv\text{Si-O}\cdot$ surface defect

	M_3/SiO_2		
	Cu	Ag	Au
E_{nucl} (eV)	-2.49 (-0.72) ^a	-1.96 (-0.48) ^a	-2.00 (-0.61) ^a
E_{adh} (eV)	-3.94	-3.04	-2.59
$Q(\text{M}_A)$ (a.u.)	0.53	0.52	0.41
$Q(\text{M}_B)$ (a.u.)	0.39	0.51	0.09
$Q(\text{M}_C)$ (a.u.)	-0.17	-0.24	0.08
$Q(\text{M}_3)$ (a.u.)	0.75	0.79	0.58
$Q(\text{O}_{\text{supp}})$ (a.u.)	-1.29	-1.30	-1.14

^a In parentheses, the E_{nucl} of free metal trimers: $E_{\text{nucl}} = [E(\text{M}_3) - E(\text{M}_1) - E(\text{M}_2)]$.

Table 4
Calculated vertical ionization potentials (IP) values (in eV) for the isolated metal particles

	IP		
	Cu	Ag	Au
M_1	7.83 (7.72) ^a	7.75 (7.57) ^a	9.42 (9.22) ^a
M_2	7.99 (7.89) ^a	7.80 (7.56) ^a	9.49 (9.16) ^c
M_3	5.76 (5.78) ^a	5.77 (~6) ^b	7.22 (7.27) ^c

Experimental IP values between brackets.

^a From ref. [27].

^b From ref. [28].

^c From ref. [29].

If now the analysis of E_{nucl} values is performed taking into account the nature of the metal, the same trend is observed for isolated and supported dimers: $\text{Cu} \approx \text{Au} > \text{Ag}$ (in magnitude). Similarly as for free dimers, the deep position of Ag d-levels in the energy scale could explain the relatively weak Ag–Ag interaction.

However, for supported M_3 the sequence in the M–M strength is slightly different: $\text{Cu} > \text{Ag} \approx \text{Au}$. This behaviour could be interpreted as follows. Two main factors take place in the M_1 – M_2 OSi \equiv bonding: (i) the interaction between two d-type orbitals and (ii) the reactivity of the $\cdot M_2$ –O–Si \equiv site due to its open-shell electronic structure to bind another M atom. For Cu, both factors are important. The spin density (SD) is mainly localized on the dimer (SD=0.84; see Table 2) yielding a strong interaction with the isolated Cu atom during the nucleation process. For Ag, the contribution (i) is relatively weak, nevertheless (ii) should be important due the high reactivity of the supported Ag_2 ; in fact, the SD values are the same as for copper. Finally, for Au the factor (i) contributes strongly to the bonding but the factor (ii) is relatively weak because the supported Au_2 has a SD value of 0.54, making this site less reactive towards the Au atom. Thus, while for Cu both factors are important, for Ag and Au only one of them contributes greatly.

3.3. Study of the metal–oxide interaction: adhesion energies

The adhesion energy is defined as the energy associated with the metal particle adsorption as a unit. The calculated

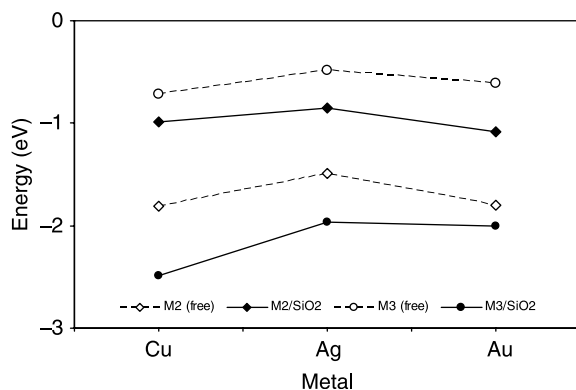


Fig. 5. Nucleation energies of Cu, Ag and Au metals as dimers and trimers adsorbed on silica defect.

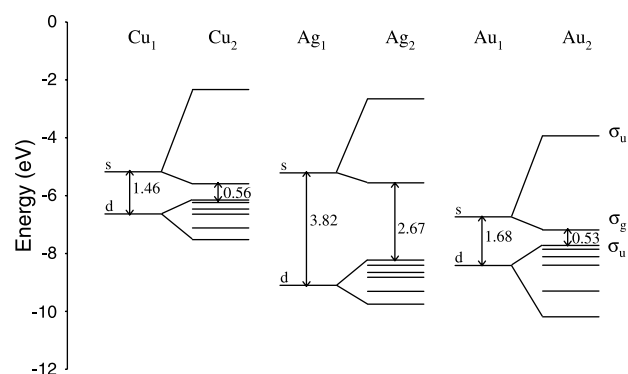


Fig. 6. Molecular orbital levels of the Cu, Ag and Au atoms and dimers.

values are shown as a diagram in Fig. 7. Comparing individually the M_n –OSi \equiv interactions we observe that, as before, the coupling of two open-shell systems ($M_1\cdot$ or $M_3\cdot + \cdot\text{O}–\text{Si}\equiv$) produces very strong bonds.

If the comparison is performed among the metals, a clear trend in the M_n –OSi \equiv bond strength is observed: $\text{Cu} > \text{Ag} > \text{Au}$. If we consider that the main component of the bonding is the $\text{M} \rightarrow \text{oxide}$ charge transfer, we would expect the sequence: $\text{Cu} \approx \text{Ag} > \text{Au}$, according to the atomic charge and IP values. However, due to the more localized Ag(d) band, the Ag(d)–O(p) interaction should be relatively weak, making this interaction less strong than expected. Analogous arguments were employed by Grönbeck and Broqvist to explain the weak adsorption of atomic Ag on a regular O site of MgO(100) [31]. They ascribed this phenomenon to a closed d shell and a large s–d splitting for Ag. Hence, for Cu both the covalent component and the $\text{Cu} \rightarrow \text{oxide}$ charge transfer contribute to the bonding. For Ag, the charge transfer is predominant, while for Au, the Au(d)–O(p) mixing is relevant.

If the present results for M_1/SiO_2 are compared with those reported previously for TiO_2 [19] and Al_2O_3 [20], we can conclude that the charge transfer to the surface takes place according to the sequence $\text{Cu} \approx \text{Ag} > \text{Au}$ for the three oxides. On the other hand, the magnitude of adhesion energies follow the order $\text{Cu} > \text{Ag} > \text{Au}$ on SiO_2 and TiO_2 , and $\text{Cu} > \text{Au} > \text{Ag}$

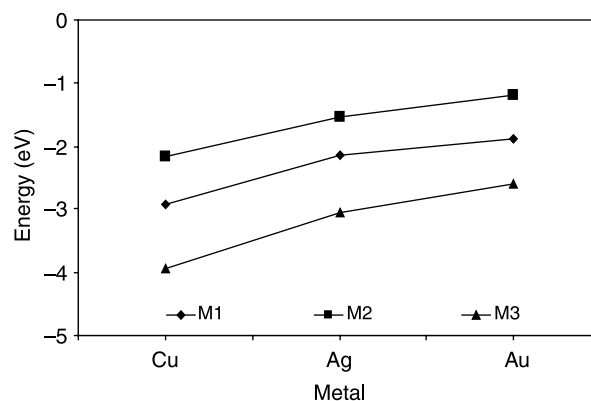


Fig. 7. Adhesion energies of Cu, Ag and Au metals as monomers, dimers and trimers adsorbed on silica defect.

on Al_2O_3 . The interaction with the surface is strong for Cu and Ag on both SiO_2 and TiO_2 with adsorption energies in the range -2.1 to -2.9 eV. For these metal atoms, a mainly covalent bond is formed on SiO_2 with a charge delocalization on the oxide surface. Conversely, Cu and Ag atoms interact mainly with the bridging oxygens of TiO_2 with formation of Cu^+ and Ag^+ ions due to a nearly full electron transfer to the oxide [19]. The adsorption of Au atom is stronger on SiO_2 ($E_{\text{adh}} \sim -1.9$ eV) than on TiO_2 ($E_{\text{adh}} \sim -0.7$ eV). On the other hand, on Al_2O_3 the metal–surface interaction is weaker than on SiO_2 and TiO_2 , with adsorption energies in the range -0.7 to -1.1 eV. On this surface, the oxygen anions become competitive with the aluminum cations for adsorbing the metal atoms. While for Cu and Ag atoms the more favored sites are the threefold hollow O sites, Au atom prefers to bind on top of the O atoms.

If the adhesion and nucleation energies are compared, a larger variation for adhesion values is observed by going from metal to metal. Thus, they can change up to 1.3 eV for M_3 , and 1.0 eV for M_1 and M_2 . Conversely, the nucleation energies present a variation interval of 0.2 eV for M_2 and 0.5 eV for M_3 . As a consequence, whereas the metal–oxide interaction clearly follows the sequence $\text{Cu} > \text{Ag} > \text{Au}$ (for M_1 , M_2 and M_3), the metal–metal interaction shows a less important variation by changing the metal.

4. Conclusions

- (i) An electronic charge transfer from the metal particle to the support occurs following the sequence: $\text{Cu} \approx \text{Ag} > \text{Au}$. The charge taken by the support resides mainly on the O of the $\equiv \text{Si}-\text{O}$ group.
- (ii) For supported Cu_2 and Cu_3 , an electrostatic interaction takes place between the terminal atom and a regular bridging O atom. For supported Ag_2 and Ag_3 , two metal atoms are directly linked with the surface O atom. In contrast, Au_2 and Au_3 interact with the surface by means of only one metal atom.
- (iii) The metal–metal (M_1-M_1 and M_2-M_1) and metal–oxide ($\text{M}_n-\text{OSi} \equiv$) interactions were analyzed from an energetic point of view. The interaction of two open-shell systems is always stronger than the interaction of an open-shell system with a closed-shell one. Particularly, for M–M interactions, the noticeable differences observed between the isolated and supported situations are mainly due to the fact that the support ‘changes’ the electronic structure of one of the interacting fragments.
- (iv) If a comparative study among the metals were performed, the bond strength of M–M interaction follows the order: $\text{Cu} \approx \text{Au} > \text{Ag}$. The deeper Ag d-type orbitals could explain the relatively weak Ag–Ag interaction. On the other hand, if the same analysis is made for the M–oxide interaction, a clear trend in the bond strength was observed: $\text{Cu} > \text{Ag} > \text{Au}$. Whereas for Au the charge transfer to the support is relatively small, for Ag the $\text{Ag}(\text{d})-\text{O}(\text{p})$ interaction should be relatively weak due to the more localized Ag(d) band.
- (v) By comparing the present results on SiO_2 with those reported for TiO_2 and Al_2O_3 , only considering the atomic adsorption, we can conclude that the charge transfer to the surface takes place according to the sequence $\text{Cu} \approx \text{Ag} > \text{Au}$ for the three oxides. The adhesion energies follow the same order $\text{Cu} > \text{Ag} > \text{Au}$ (in magnitude) only for SiO_2 and TiO_2 .

Acknowledgements

Financial support from CONICET and *Universidad Nacional del Sur* are gratefully acknowledged.

References

- [1] D.B. Clarke, A.T. Bell, *J. Catal.* 154 (1995) 314.
- [2] I.A. Fisher, A.T. Bell, *J. Catal.* 178 (1998) 153.
- [3] S.C. Kim, *J. Hazard. Mater.* B91 (2002) 285.
- [4] R.A. Koeppel, J.T. Wehrli, M.S. Wainwright, D.L. Trimm, N.W. Cant, *Appl. Catal. A* 120 (1994) 163.
- [5] M. Richter, U. Bentrup, R. Eckelt, M. Schneider, M.M. Pohl, R. Fricke, *Appl. Catal. B: Environ.* 51 (2004) 261.
- [6] P.W. Park, C.L. Boyer, *Appl. Catal. B: Environ.* 59 (2005) 27.
- [7] M. Haruta, *Catal. Today* 36 (1997) 153.
- [8] F. Gauthard, F. Epron, J. Barbier, *J. Catal.* 220 (2003) 182.
- [9] K. Persson, A. Ersson, K. Jansson, N. Iverlund, S. Jaras, *J. Catal.* 231 (2005) 139.
- [10] N. Lopez, F. Illas, G. Pacchioni, *J. Phys. Chem. B* 103 (1999) 1712.
- [11] N. Lopez, G. Pacchioni, F. Maseras, F. Illas, *Chem. Phys. Lett.* 294 (1998) 611.
- [12] N. Lopez, F. Illas, G. Pacchioni, *J. Am. Chem. Soc.* 121 (1999) 813.
- [13] M. Brause, D. Ochs, J. Günster, T. Mayer, B. Braun, V. Puchin, W. Maus-Friedrichs, W. Kempter, *Surf. Sci.* 383 (1997) 216.
- [14] V.A. Radsig, *Chem. Phys. Rep.* 14 (1995) 1206.
- [15] R.M. Ferullo, N.J. Castellani, *J. Mol. Catal. A: Chem.* 221 (2004) 155.
- [16] N. Lopez, F. Illas, G. Pacchioni, *J. Phys. Chem. B* 103 (1999) 8552.
- [17] R.M. Ferullo, N.J. Castellani, *J. Mol. Catal. A: Chem.* 234 (2005) 121.
- [18] P. Pietrzyk, *J. Phys. Chem. B* 109 (2005) 10291.
- [19] L. Giordano, G. Pacchioni, T. Bredow, J. Fernández Sanz, *Surf. Sci.* 471 (2001) 21.
- [20] N. Cruz Hernández, J. Graciani, A. Márquez, J. Fernández Sanz, *Surf. Sci.* 575 (2005) 189.
- [21] A.D. Becke, *J. Chem. Phys.* 98 (1993) 5648.
- [22] N.R. Kestner, J.E. Combariza, in: K.B. Lipkowitz, D.B. Boyd (Eds.), *Reviews in Computational Chemistry*, vol. 13, Wiley–VCH, New York, 1999, p. 99. (Chapter 2).
- [23] A.E. Reed, L.A. Curtiss, F. Weinhold, *Chem. Rev.* 88 (1988) 899.
- [24] I.N. Levine, *Quantum Chemistry*, fifth ed., Prentice Hall, New Jersey, 2000 p. 505.
- [25] M.J. Frisch, G.W. Trucks, H.B. Schlegel, G.E. Scuseria, M.A. Robb, J.R. Cheeseman, J.A. Montgomery Jr., T. Vreven, K.N. Kudin, J.C. Burant, J.M. Millam, S.S. Iyengar, J. Tomasi, V. Barone, B. Mennucci, M. Cossi, G. Scalmani, N. Rega, G.A. Petersson, H. Nakatsuji, M. Hada, M. Ehara, K. Toyota, R. Fukuda, J. Hasegawa, M. Ishida, T. Nakajima, Y. Honda, O. Kitao, H. Nakai, M. Klene, X. Li, J.E. Knox, H.P. Hratchian, J.B. Cross, C. Adamo, J. Jaramillo, R. Gomperts, R.E. Stratmann, O. Yazyev, A.J. Austin, R. Cammi, C. Pomelli, J.W. Ochterski, P.Y. Ayala, K. Morokuma, G.A. Voth, P. Salvador, J.J. Dannenberg, V.G. Zakrzewski, S. Dapprich, A.D. Daniels, M.C. Strain, O. Farkas, D.K. Malick, A.D. Rabuck, K. Raghavachari, J.B. Foresman, J.V. Ortiz, Q. Cui, A.G. Baboul, S. Clifford, J. Cioslowski, B.B. Stefanov, G. Liu, A. Liashenko, P. Piskorz, I. Komaromi, R.L. Martin, D.J. Fox, T. Keith, M.A.

- Al-Laham, C.Y. Peng, A. Nanayakkara, M. Challacombe, P.M.W. Gill, B. Johnson, W. Chen, M.W. Wong, C. Gonzalez, J.A. Pople, GAUSSIAN 03, Revision C.02, Gaussian, Inc., Wallingford, CT, 2004.
- [26] J.M. Antonietti, M. Michalski, U. Heiz, H. Jones, K. Lim, N. Rösch, A. Del Vitto, G. Pacchioni, Phys. Rev. Lett. 94 (2005) 213402.
- [27] M.D. Morse, Chem. Rev. 86 (1986) 1049.
- [28] D.W. Boo, Y. Ozaki, L.H. Andersen, W.C. Lineberger, J. Phys. Chem. A 101 (1997) 6688.
- [29] M.A. Cheeseman, J.R. Eyster, J. Phys. Chem. 96 (1992) 1082.
- [30] X. Wang, X. Wan, H. Zhou, S. Takami, M. Kubo, A. Miyamoto, J. Mol. Struct. (Theochem) 579 (2002) 221.
- [31] H. Grönbeck, P. Broqvist, J. Phys. Chem. B 107 (2003) 12239.